IEEE Access
Multidisciplinary | Rapid Review | Open Access Journal

Received August 1, 2018, accepted September 26, 2018, date of publication October 10, 2018, date of current version November 8, 2018.

Digital Object Identifier 10.1109/ACCESS.2018.2875123

An Ultrasonic Guided Wave Mode Excitation Method in Rails

XU XINING[1,2], ZHUANG LU[1], XING BO[1], YU ZUJUN[1,2], AND ZHU LIQIANG[1,2]

[1]School of Mechanical, Electronic, and Control Engineering, Beijing Jiaotong University, Beijing 100044, China
[2]Key Laboratory of Vehicle Advanced Manufacturing, Measuring, and Control Technology, Ministry of Education, Beijing Jiaotong University, Beijing 100044, China

Corresponding author: Yu Zujun (zjyu@bjtu.edu.cn)

This work was supported by the National Key Research and Development Program of China, Supported by Foundation of Key Laboratory of Vehicle Advanced Manufacturing, Measuring, and Control Technology, Ministry of Education, Beijing Jiaotong University, China, under Grant 2016YFB1200401.

ABSTRACT This paper proposes a new method for exciting a specific mode of guided ultrasonic wave in a rail. The method requires the cross-sectional mode shape to determine excitation direction, excitation coefficient, and excitation position of each mode. The cross-sectional mode shape data of all modes are acquired by the semi-analytical finite element (SAFE) method. The optimum excitation direction is obtained by solving the Euclidean distance between different modes. According to the shape feature of a rail, the cross section of a rail is divided into three segments, including the rail base, the rail web, and the rail head. The excitation coefficients are obtained by analyzing vibration characteristics in these three segments. The covariance matrix of each mode at a specific frequency is established, and the result is used to obtain the best excitation point. The response to an excitation in the rail can then be computed by the SAFE method. It has been verified that the excitation method proposed in this paper can excite a specific ultrasonic-guided wave mode at the low frequency of 200 Hz and the high frequency of 35 kHz, respectively.

INDEX TERMS Excitation response, Fourier transform, semi-analytical finite element, ultrasonic guided wave.

I. INTRODUCTION

Ultrasonic guided wave is a kind of special ultrasonic waves generated by continuous reflection and refraction with the border of waveguide and conversion of vertical and horizontal waves when propagates in the waveguide including rods, pipelines, plates, and rails [1]. The guided ultrasonic wave propagates farther than the ultrasonic bulk wave, and it covers the whole cross section of waveguides. Therefore, the detection efficiency of ultrasonic guided wave is higher than the ultrasonic bulk wave and it is more suitable for non-destructive testing of long distance waveguides, such as plates, pipelines, and rails.

Compared with other fault diagnosis techniques [2], ultrasonic guided waves have the characteristics of long detection distance. In the study on the defect detection based on ultrasonic guided wave, quite a few scholars have developed specific probes to excite specific modes for detection. According to the different characteristics of ultrasonic guided waves at low frequency and high frequency, Khalili and Cawley [3] investigates the relative ability of angled piezoelectric and meander coil EMAT probes to produce single-mode transduction in the medium and high frequency-thickness regions of the dispersion curves. The omni-directional S0 mode magnetostrictive transducers developed by Liu *et al.* [4] constituted a sparse sensor array, which was used to locate the defects in the plate structure. In the detection of pipeline defects, the dispersion SH1 mode was generated by Andruschak *et al.* [5] with an electromagnetic acoustic transducer. It was used to detect hidden corrosion defects on the pipeline support interface.

In terms of the stress measurement based on ultrasonic guided wave, the researchers found that the stress-sensitive modes are suitable for rail stress measurement. Xu [6] from Beijing Jiaotong University proposed an indicator model of ultrasonic guided wave mode in rail stress measurement. The results manifested that the guided wave mode selected according to the maximum value of index model was more sensitive to rail stress. Furthermore, Javadi *et al.* [7] used longitudinal critically refracted waves to test the residual stress generated by austenitic stainless steel during the welding process, and compared with the finite element calculation results, which has good consistency.

However, due to the complexity of the cross section of a rail, the ultrasonic guided wave has a variety of modes in process of propagating. The propagating speed, vibration form, attenuation coefficient, and other properties of all modes are different. Thus, detection objects applicable to all modes are different. When the ultrasonic guided wave technology is applied to detect internal defects of a rail, the energy of the different modes can be concentrated on rail head, rail web, rail base, and the whole cross section of rail, respectively. Therefore, the specific mode will be selected according to position of detected defects. It is particularly important to study the excitation method of a specific mode in rails.

When the excitation methods of specific guided wave mode are investigated, a host of scholars have done a multitude of research on regular cross section waveguides, such as plates [8], [9], pipelines [10]–[13], etc. On the one hand, based on phase control technology, Pelts *et al.* [14] adopted comb transducer by setting quantity, space, size, excitation pulse sequence, and other parameters of transducer to excite the specific mode. Afterwards, this method was applied to intensify interested modes and proved by an ocean of simulations. Wu *et al.* [15] excited single S0 and A0 mode on plates by loading displacements on finite element model according to wave structure of the corresponding mode. Moreover, Huyg *et al.* [16] restrained generation of some modes and increased energy of excitation signal by optimizing different connection types of electromagnetic-acoustic array elements. In addition, aiming at the surface defect detection of the thick-walled pipe [17], a PZT based the flexible comb Rayleigh wave transducer was proposed by He Cunfu *et al.* The experimental result demonstrated that the comb Rayleigh wave transducers possessed good directivity. On the other hand, using time delay technology, Kannajosyula *et al.* [18] succeed in one-way exciting and receiving guided wave mode. Subsequently, Borigo *et al.* [19] adopted annular transducer array to excite the omni-directional guided wave in steel plate. What's more, Rose [20] designed multi-channel time delay control system to excite the specific mode in pipeline by controlling time difference in transducer array. All these results demonstrated that it is paramount to excite the specific modes for detection.

As the cross sections of plates and pipelines are regular, the types of modes are correspondingly less. Accordingly, the mode is easily selected and controlled by the phase and time control. However, the control is relatively difficult while the cross section of a rail is complicated and the types of modes are various. It is of great significance to excite a single mode which is sensitive to defects or stress of rails by using a specific excitation method. Therefore, this paper will focus on the research on the excitation method of guided wave modes in rails, and the excitation direction, excitation coefficient, and excitation point of each mode are determined on the basis of vibration characteristics and correlations of each guided mode.

In this paper, we propose a new method for exciting a specific mode of guided ultrasonic wave in a rail. Firstly, the Euclidean distance is used to calculate the actual distance between the vibration displacement vectors of different modes in a rail to select the optimal excitation direction. Then, the excitation coefficient is calculated according to the magnitude of the vibration displacement of different modes. And the covariance equation is used to describe the vibration characteristics of different nodes of the same mode to determine the best excitation node. After that, considering the amplitude of the excitation signal and the interference of other mode, the optimal reception direction of the excitation signal is selected. Finally, the excitation response calculation method is used to verify the excitation of the specific mode of the CHN60 rail at low frequency 200 Hz and high frequency 35 kHz.

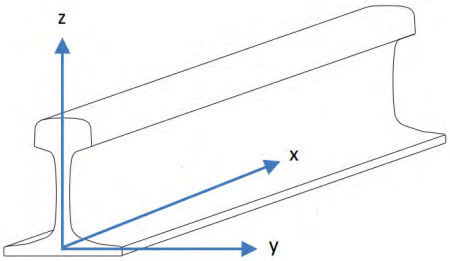

FIGURE 1. Coordinates of CHN60 rail.

II. SEMI-ANALYTICAL FINITE ELEMENT (SAFE) METHOD

In order to study excitation methods of all modes for ultrasonic guided wave in a rail, vibration mode information about all modes is required. Therefore, the SAFE method will be adopted and it is an extremely simple and effective method which is most frequently used to obtain the dispersion curve of guided wave in waveguide [21], [22] and it is proved that the method can be applied to obtain dispersion curve of plate, pole, pipeline, and rail. The wave equation of guided wave in a rail is established to solve the problem of general eigenvalue and to determine the relationship between wave number and frequency. The eigenvector includes vibration form information of guided wave mode. In this paper, CHN60 rail is taken as an example to illustrate the process of adopting the SAFE method to obtain the vibration form information of the rail. As shown in Fig. 1, the coordinate system of the rail is established as follows.

Displacement, stress, and strain of each point in the rail can be expressed as [23]:

$$\begin{aligned} \boldsymbol{u} &= \begin{bmatrix} u_x & u_y & u_z \end{bmatrix}^T \\ \boldsymbol{\sigma} &= \begin{bmatrix} \sigma_x & \sigma_y & \sigma_z & \sigma_{yz} & \sigma_{xz} & \sigma_{xy} \end{bmatrix}^T \\ \boldsymbol{\varepsilon} &= \begin{bmatrix} \varepsilon_x & \varepsilon_y & \varepsilon_z & \gamma_{yz} & \gamma_{xz} & \gamma_{xy} \end{bmatrix}^T \end{aligned} \tag{1}$$

The elastic constant matrix of the rail is expressed in $\boldsymbol{C}$ and the stress can be calculated according to elastic constant

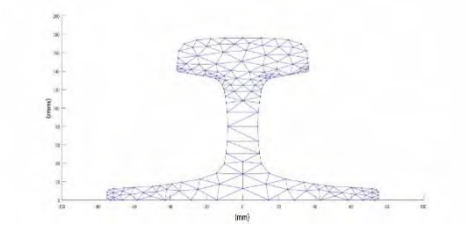

FIGURE 2. Discretization of triangle elements.

matrix and strain, namely: $\sigma = \boldsymbol{C}\boldsymbol{\varepsilon}$ [23].

$$\boldsymbol{\varepsilon} = \left[\boldsymbol{L}_x \frac{\partial \boldsymbol{u}}{\partial x} + \boldsymbol{L}_y \frac{\partial \boldsymbol{u}}{\partial y} + \boldsymbol{L}_z \frac{\partial \boldsymbol{u}}{\partial z}\right] \tag{2}$$

Where:

$$\boldsymbol{L}_x = \begin{bmatrix} 1 & 0 & 0 \\ 0 & 0 & 0 \\ 0 & 0 & 0 \\ 0 & 0 & 0 \\ 0 & 0 & 1 \\ 0 & 1 & 0 \end{bmatrix}, \quad \boldsymbol{L}_y = \begin{bmatrix} 0 & 0 & 0 \\ 0 & 1 & 0 \\ 0 & 0 & 0 \\ 0 & 0 & 1 \\ 0 & 0 & 0 \\ 1 & 0 & 0 \end{bmatrix},$$

$$\boldsymbol{L}_z = \begin{bmatrix} 0 & 0 & 0 \\ 0 & 0 & 0 \\ 0 & 0 & 1 \\ 0 & 1 & 0 \\ 1 & 0 & 0 \\ 0 & 0 & 0 \end{bmatrix} \tag{3}$$

When the SAFE method is adopted to obtain the frequency dispersion curve of ultrasonic guided wave in CHN60 rail, it is assumed that the ultrasonic guided wave propagates in the rail in longitudinal direction by means of simple harmonic vibration and the finite element dispersion is only carried out for cross section of the rail. The displacement field of the cross-sectional plane in the rail can be expressed [23] by Equation (4):

$$\boldsymbol{u}(x, y, z, t) = \begin{bmatrix} u_x(x, y, z, t) \\ u_y(x, y, z, t) \\ u_z(x, y, z, t) \end{bmatrix} = \begin{bmatrix} U_x(y, z) \\ U_y(y, z) \\ U_z(y, z) \end{bmatrix} e^{i(\xi x - \omega t)} \tag{4}$$

The ω is frequency and ξ is wave number.

The cross section of the rail is discretized by triangular elements, as is shown in Fig. 2.

The displacement of any point in element can be determined according to the nodal displacement and shape function. The strain vector of element can be expressed by nodal displacement. According to strain and displacement, the strain energy and potential energy of any point in CHN60 rail can be determined and substituted into equations of Hamilton Principle to deduce ordinary homogeneous wave equation of guided wave [23]:

$$\left[\boldsymbol{K}_1 + i\xi\boldsymbol{K}_2 + \xi^2\boldsymbol{K}_3 - \omega^2\boldsymbol{M}\right]_M \boldsymbol{U} = 0 \tag{5}$$

The $\boldsymbol{K}_1$, $\boldsymbol{K}_2$, $\boldsymbol{K}_3$ are 3 stiffness matrixes, ξ and ω respectively are wave number and frequency, $\boldsymbol{M}$ and $\boldsymbol{U}$ respectively are mass matrix and nodal displacement vector.

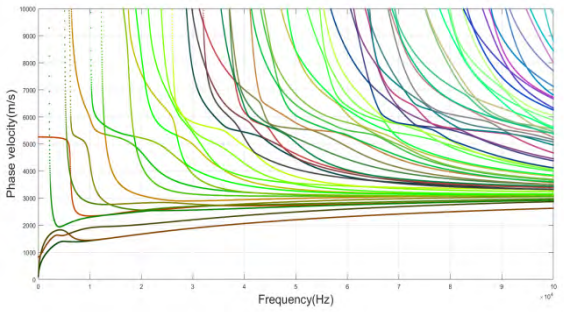

FIGURE 3. Phase velocity dispersion curves.

TABLE 1. Rail's phase velocity and group velocity values at 200 Hz.

No.	Mode	Phase velocity value	Group velocity value
1	Flexural horizontal mode	403m/s	772m/s
2	Flexural vertical mode	634m/s	1218m/s
3	Torsional mode	847m/s	886m/
4	Extensional mode	5263m/s	5263m/s

According to Equation (5), the method of determining ordinary eigenvalue can be used to determine corresponding ξ value based on frequency ω and then draw the frequency dispersion curve of ultrasonic guided wave in CHN60 rail, as is shown in Fig. 3.

It can be seen that there are various propagating modes existence in the same frequency of the rail. With the gradual increase of frequency, the number of guided wave modes propagating in the rail will gradually increase. The equation (5) can be used to determine eigenvalues ξ and ω as well as eigenvector $\hat{\boldsymbol{U}}$. The eigenvalue reflects dispersion features of ultrasonic guided wave and eigenvector represents vibration form of the mode. In low frequency, there are less modes. When the frequency is 200 Hz, there are 4 modes of ultrasonic guided wave in CHN60 rail. Phase velocity and group velocity values of all modes are shown in Table 1.

The vibration mode diagram for each mode can be drawn according to eigenvector $\hat{\boldsymbol{U}}$. When the existing frequency is $f = 200Hz$, ω value can be determined and then $\boldsymbol{K}_1$, $\hat{\boldsymbol{K}}_2$, $\boldsymbol{K}_3$, ω, $\boldsymbol{M}$ will be substituted in Equation (5) to determine feature equation. In this way, we can know eigenvalue ξ and eigenvector $\hat{\boldsymbol{U}}$. Eigenvector $\hat{\boldsymbol{U}}$ represents displacement of all nodes after dispersion on cross section of the rail. Fig. 4 (a-d) show respectively vibration mode diagrams of 4 modes in which the cross section of the rail at left side is in original size and the right side is the sectional view of vibration mode of the mode.

Mode 1, the whole cross section rotates along the vertical axis. Thus, the mode is the flexural horizontal mode. Mode 2, turning over back and forth along rail base, it is the flexural vertical mode. Mode 3 is the torsional mode. Mode 4 is extensional mode. The three-dimensional diagram for vibration form of all modes is shown in Fig. 5.

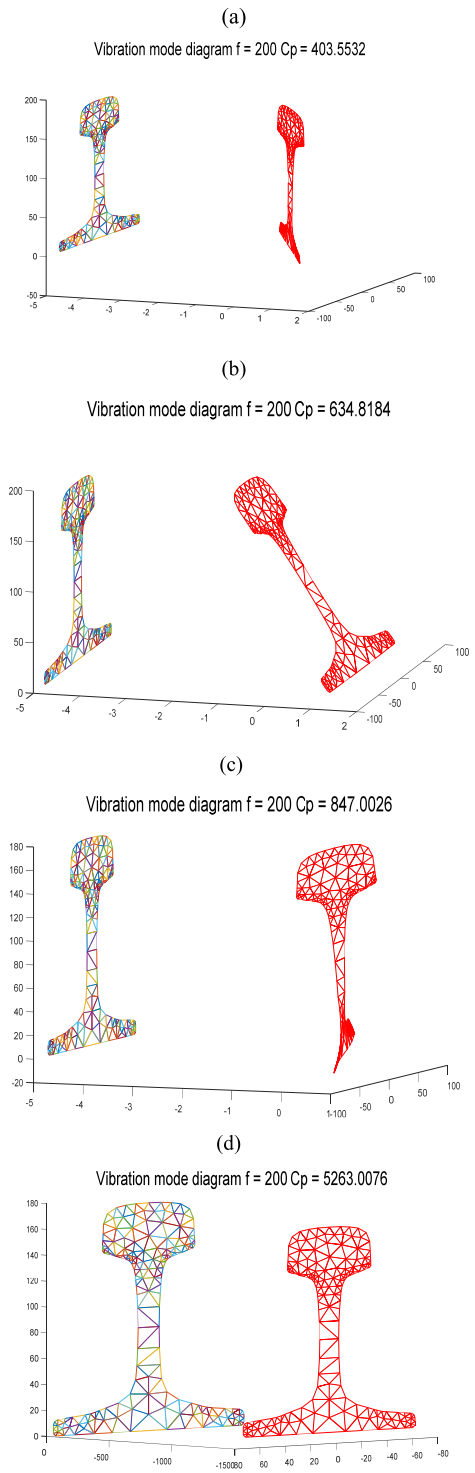

FIGURE 4. Cross sectional mode shapes at 200 Hz. The phase velocity of flexural horizontal mode is (a), 403 m/s. The phase velocity of flexural vertical mode is (b), 634 m/s. The phase velocity of torsional mode is (c), 847 m/s. And the phase velocity of extensional mode is (d), 5263 m/s.

In high frequency, there are many modes. When the frequency is 35 kHz, there are 20 modes of ultrasonic guided wave in CHN60 rail and phase velocity and group velocity values of all modes are shown in Table 2.

Fig. 6 is vibration mode diagrams of 20 modes.

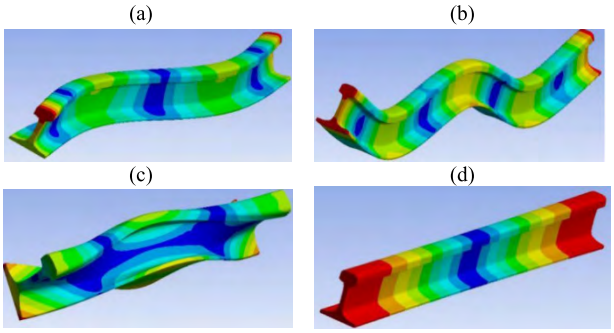

FIGURE 5. CHN60 Rail's modesat low frequency. (a) Flexural horizontal mode. (b) Flexural vertical mode. (c) Torsional mode. (d) Extensional mode.

TABLE 2. Rail's phase velocity and group velocity values at 35KHz.

No.	Phase velocity value	Group velocity value
1	1983.80m/s	2852.71m/s
2	1984.05m/s	2850.88m/s
3	2286.06m/s	3019.87m/s
4	2592.53m/s	2840.10 m/s
5	2725.71m/s	2788.97 m/s
6	2743.72m/s	2658.34 m/s
7	2737.57m/s	3215.14 m/s
8	2919.28m/s	3098.60 m/s
9	3104.71m/s	2924.14 m/s
10	3297.15m/s	2704.92m/s
11	3389.87m/s	2230.95m/s
12	3708.61m/s	2418.10 m/s
13	4194.78m/s	1795.76 m/s
14	4167.81m/s	2146.20 m/s
15	4955.74m/s	2879.74 m/s
16	5554.76m/s	4266.58 m/s
17	5862.23m/s	2712.24 m/s
18	6796.88m/s	2650.07 m/s
19	6415.38m/s	2692.66 m/s
20	8155.23m/s	3402.45 m/s

The SAFE method can be used to obtain the vibration mode information of all guided wave modes in the rail. Excitation direction, excitation coefficient, and excitation points of all modes can be determined according to displacement of all nodes in vibration mode, analysis of vibration features, and relevant features of all modes.

III. THE EXCITED RESPONSE CACULATION METHOD

In order to verify that the selected excitation direction, excitation coefficient, and excitation point can excite a specific mode, the excitation response calculation or ANSYS finite element software is used for simulation. Due to the long simulation time of ANSYS, the excitation response calculation method is used in this paper. Firstly, the Fourier transform

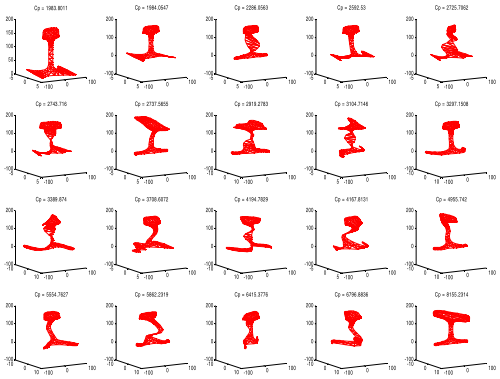

FIGURE 6. Cross sectional mode shapes at 35 kHz.

was conducted to the excitation signal applied on the rail to obtain the frequency domain value $\widehat{F}(j\omega)$. Secondly, the system function model $\boldsymbol{H}(j\omega)$ of the rail was established by the SAFE method, and the response result of the excitation signal in the frequency domain was solved by $\boldsymbol{V}(j\omega) = \widehat{F}(j\omega) \cdot \boldsymbol{H}(j\omega)$. Finally, the Fourier inversion was conducted to $\boldsymbol{V}(j\omega)$ to obtain the response result of applying an excitation signal at a specified position of the rail. The modelling process is described as follows.

The system function model [24] of the rail is expressed by Equation (6):

$$\boldsymbol{H}(y,z,f) = \sum_{m=1}^{2M} -\frac{\boldsymbol{U}_m^L \tilde{\boldsymbol{p}}}{\boldsymbol{B}_m} \boldsymbol{U}_m^{Rup} e^{i[\xi_m(x-x_S)]} \tag{6}$$

Where:

y : horizontal ordinate of cross section of rail;

z : vertical coordinate of cross section of rail;

f : vibration frequency of ultrasonic guided wave in rail;

m : label of ultrasonic guided wave mode; there are 2m guided waves;

x_S : coordinate value of applying excitation signal point at x direction;

$\tilde{\boldsymbol{p}}$: amplitude of applying excitation signal;

$\boldsymbol{U}_m^L$: left eigenvector of ultrasonic guided wave vibration mode;

$\boldsymbol{U}_m^{Rup}$: upper half of right eigenvector of ultrasonic guided wave vibration mode;

$\boldsymbol{B}_m$ and $\boldsymbol{B}$ in Equation (6) can be calculated [23], [24] by Equation (7) and (8).

$$\boldsymbol{B}_m = \boldsymbol{U}_m^L \boldsymbol{B} \boldsymbol{U}_m^R \tag{7}$$

$$\boldsymbol{B} = \begin{bmatrix} \boldsymbol{K}_1 - \omega^2 \boldsymbol{M} & 0 \\ 0 & -\boldsymbol{K}_3 \end{bmatrix} \tag{8}$$

The $\boldsymbol{K}_1$ and $\boldsymbol{K}_3$ are stiffness matrix in the general homogenization wave equation of the ultrasonic guided wave.

Fourier transform is performed to the excitation signal $F(t)$:

$$\widehat{F}(f) = \int_{-\infty}^{\infty} F(t)\, e^{-i2\pi ft} dt \tag{9}$$

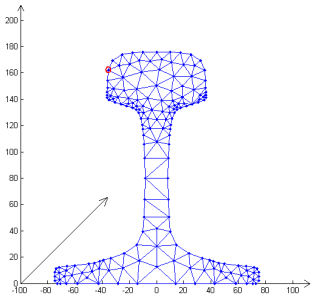

FIGURE 7. Cross section of CHN60 rail after discrete triangle elements.

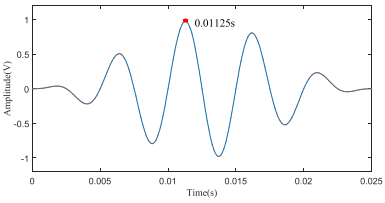

FIGURE 8. Excitation signal.

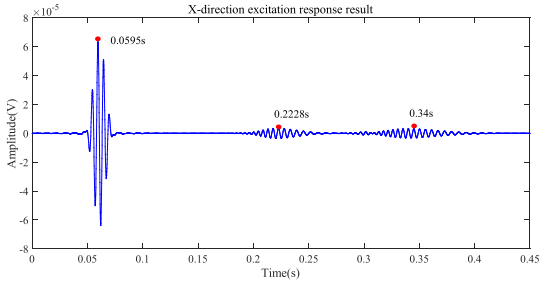

FIGURE 9. X-direction excitation response result.

$\boldsymbol{V}(y,z,f)$ can be obtained by convolution calculation [24]:

$$\begin{aligned} \boldsymbol{V}(y,z,f) &= \widehat{F}(f) \cdot \boldsymbol{H}(y,z,f) \\ &= \widehat{F}(f) \cdot \sum_{m=1}^{M} -\frac{\boldsymbol{U}_m^L \tilde{\boldsymbol{p}}}{\boldsymbol{B}_m} \boldsymbol{U}_m^{Rup} e^{i[\xi_m(x-x_S)]} \end{aligned} \tag{10}$$

The Fourier inversion is performed for $\boldsymbol{V}(y,z,f)$ to obtain the response result of excitation signal.

A point is randomly selected on the rail head as an excitation point, as shown in Fig 7, and an excitation signal is applied along the x direction at the node A of the red area in the Fig 7.

The excitation signal is a sine wave modulated by Hanning window with a frequency of 200 Hz. The peak value of the signal appears at 0.01125 seconds. The waveform of the excitation signal is shown in Fig 8.

The final excitation response result can be obtained by the calculation method of excitation response, as shown in Fig 9.

Three time-domain signal waveforms appear in the Fig 9. That is to say, three modes are generated when the signal is applied at the node A along the x direction. The peak time of mode signal appears at $t_1 = 0.0595$s, $t_2 = 0.2228$s, and $t_3 = 0.34$s, respectively. According to the time difference

TABLE 3. Group velocity values of three modes are excited in x direction.

Excitation time	Response time	Group velocity value	Mode
0.01125s	0.0595s	5181m/s	Extensional mode
0.01125s	0.2228s	1181m/s	Flexural vertical mode
0.01125s	0.34s	760m/s	Flexural horizontal mode

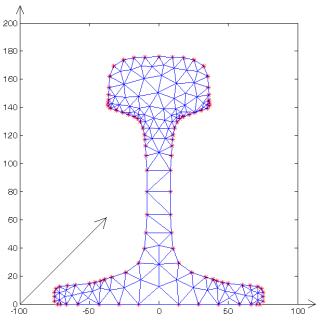

FIGURE 10. All external feature nodes.

from the excitation signal and the simulation distance, the group velocity values of the three modes can be obtained, as shown in Table 3.

If the excitation is applied randomly, multiple modes may appear and it will increase the difficulties to subsequent signal analysis. Therefore, it is necessary to select an appropriate excitation method and control the quantity of modes that are excited. In this paper, the excitation position, excitation coefficient, and excitation direction of all modes are determined by analyzing the vibration mode information of each mode, calculating the Euclidean distance and covariance of each mode shape data.

IV. THE EXCITATION METHOD OF ULTRASONIC GUIDED WAVE MODE

A. DETERMINE THE EXCITATION DIRECTION

When the rail is applied excitation, it can only be applied on external nodes of the rail and all excitation nodes outside cross section of the rail can be defined as feature nodes of the mode, as is shown in Fig. 10. All feature nodes are marked with asterisk.

Total number of all nodes outside cross section of the rail is p, each node has degree of freedom in three directions and the displacements of each degree of freedom are respectively recorded as x_i, y_i, z_i.

The rail has k modes in excitation with frequency of f, the displacement vector of 3 degrees of freedom in the mode m feature point can be expressed as:

$$X_m = \begin{bmatrix} x_{1m} & x_{2m} & \dots & x_{pm} \end{bmatrix}^T \tag{11}$$

$$Y_m = \begin{bmatrix} y_{1m} & y_{2m} & \dots & y_{pm} \end{bmatrix}^T \tag{12}$$

$$Z_m = \begin{bmatrix} z_{1m} & z_{2m} & \dots & z_{pm} \end{bmatrix}^T \tag{13}$$

The feature points start from the center of rail base and they will be successively listed along clockwise direction. There are 97 external nodes in all, namely p=97.

The Euclidean distance can be used to describe the actual distance between modes in three-dimensional space [25]. The Euclidean distance of mode m and mode n in x direction in cross section of the rail can be defined as:

$$X\rho_{mn} = \sqrt{\sum_{i=1}^{p} (x_{im} - x_{in})^2} \tag{14}$$

The Euclidean distance matrix in x direction can be generated:

$$X\rho = \begin{bmatrix} X\rho_{11} & X\rho_{12} & \cdots & \cdots & X\rho_{1k} \\ X\rho_{21} & X\rho_{22} & \cdots & \cdots & X\rho_{2k} \\ & & \ddots & & \\ & & & \ddots & \\ X\rho_{k1} & X\rho_{k2} & \cdots & \cdots & X\rho_{kk} \end{bmatrix} \tag{15}$$

The Euclidean distance matrix in y direction:

$$Y\rho = \begin{bmatrix} Y\rho_{11} & Y\rho_{12} & \cdots & \cdots & Y\rho_{1k} \\ Y\rho_{21} & Y\rho_{22} & \cdots & \cdots & Y\rho_{2k} \\ & & \ddots & & \\ & & & \ddots & \\ Y\rho_{k1} & Y\rho_{k2} & \cdots & \cdots & Y\rho_{kk} \end{bmatrix} \tag{16}$$

The Euclidean distance matrix in z direction:

$$Z\rho = \begin{bmatrix} Z\rho_{11} & Z\rho_{12} & \cdots & \cdots & Z\rho_{1k} \\ Z\rho_{21} & Z\rho_{22} & \cdots & \cdots & Z\rho_{2k} \\ & & \ddots & & \\ & & & \ddots & \\ Z\rho_{k1} & Z\rho_{k2} & \cdots & \cdots & Z\rho_{kk} \end{bmatrix} \tag{17}$$

The Euclidean distance for k modes of the rail in x, y, and z directions with excitation of frequency f can be calculated. The Euclidean distances of mode m in x, y, and z directions are compared and the direction with maximum Euclidean distance will be selected to be the best excitation direction of mode m.

1) DETERMINE THE EXCITATION DIRECTION AT 200 Hz

In the low frequency domain, there are less modes in the rail. Taking 200 Hz as an example, the excitation direction of 4 modes will be calculated as follows.

When the frequency is 200 Hz, vibration displacement of 97 nodes in 4 modes in x, y, and z directions will be substituted into Equation (15), (16), and (17) to determine Euclidean distance matrixes in three directions.

The Euclidean distance matrix in in x direction:

$$X\rho = \begin{bmatrix} 0 & 0.0462 & 0.0232 & 0.7205 \\ 0.0462 & 0 & 0.0448 & 0.7234 \\ 0.0232 & 0.0448 & 0 & 0.7204 \\ 0.7205 & 0.7234 & 0.7204 & 0 \end{bmatrix} \tag{18}$$

TABLE 4. The average value of Euclidean distance in x, y, and z directions at 200 Hz.

Mode	x	y	z
Flexural horizontal mode	0.2633	0.2890	0.1970
Flexural vertical mode	0.2715	0.1933	0.3546
Torsional mode	0.2628	0.3800	0.2889
Extensional mode	0.7214	0.1933	0.1911

The Euclidean distance matrix in y direction:

$$Y\rho = \begin{bmatrix} 0 & 0.2204 & 0.4263 & 0.2204 \\ 0.2204 & 0 & 0.3569 & 0.0028 \\ 0.4263 & 0.3569 & 0 & 0.3569 \\ 0.2204 & 0.0028 & 0.3569 & 0 \end{bmatrix} \quad (19)$$

The Euclidean distance matrix in z direction:

$$Z\rho = \begin{bmatrix} 0 & 0.3320 & 0.2416 & 0.0174 \\ 0.3320 & 0 & 0.4004 & 0.3314 \\ 0.2416 & 0.4004 & 0 & 0.2246 \\ 0.0174 & 0.3314 & 0.2246 & 0 \end{bmatrix} \quad (20)$$

The average value of Euclidean distances in x, y, and z directions will be calculated for 4 modes.

In Table 4, when the frequency is 200 Hz, the average value of Euclidean distances for 4 modes in x, y, and z directions will be analyzed and the direction with maximum Euclidean distance will be selected as excitation direction. Therefore, excitation in y direction will be selected for flexural horizontal mode, excitation in z direction will be selected for flexural vertical mode, excitation in y direction will be selected for torsional mode and excitation in x direction will be selected for extensional mode.

2) DETERMINE THE EXCITATION DIRECTION AT 35 kHz

In high frequency, there are many modes in the rail. Subsequently the excitation direction of 20 modes will be calculated when the frequency is 35 kHz.

Vibration displacement of 97 nodes in 20 modes in x, y, and z directions will be substituted into Equation (15), (16), and (17) to determine Euclidean distance matrixes in three directions. Besides, the average value of Euclidean distance in x, y, and z directions will be calculated for 20 modes.

The average value of Euclidean distance in y direction will be calculated for 20 modes.

The average value of Euclidean distance in z direction will be calculated for 20 modes.

There are many modes in 35 kHz and therefore mode 1, mode 3, and mode 10 are randomly selected in this paper for verification. The average of Euclidean distance for 3 modes in x, y, and z directions when the frequency in Table 5, 6, and 7 is 35 kHz will be analyzed and the direction with maximum Euclidean distance will be selected as excitation direction. Therefore, excitation in z direction is selected for mode 1, excitation in y direction is selected for mode 3 and excitation in y direction is selected for mode 10.

TABLE 5. The average value of Euclidean distance in x direction at 35 kHz.

No.	x	No.	x
1	0.0113	11	0.0130
2	0.0113	12	0.0118
3	0.0123	13	0.0143
4	0.0115	14	0.0128
5	0.0117	15	0.0160
6	0.0115	16	0.0260
7	0.0118	17	0.0236
8	0.0120	18	0.0254
9	0.0116	19	0.0214
10	0.0131	20	0.0338

TABLE 6. The average value of Euclidean distance in Y direction at 35 kHz.

No.	y	No.	y
1	0.0096	11	0.0160
2	0.0096	12	0.0124
3	0.0145	13	0.0188
4	0.0103	14	0.0129
5	0.0124	15	0.0175
6	0.0120	16	0.0114
7	0.0096	17	0.0135
8	0.0138	18	0.0134
9	0.0133	19	0.0231
10	0.0169	20	0.0148

TABLE 7. The average value of Euclidean distance in Z direction at 35 kHz.

No.	z	No.	z
1	0.0128	11	0.0116
2	0.0127	12	0.0200
3	0.0100	13	0.0131
4	0.0145	14	0.0183
5	0.0126	15	0.0109
6	0.0138	16	0.0145
7	0.0139	17	0.0202
8	0.0115	18	0.0098
9	0.0141	19	0.0169
10	0.0102	20	0.0112

B. DETERMINE THE EXCITATION COEFFICIENT

The cross-sectional shape of the rail is complex and there are many propagating guided wave modes in the rail and different guided wave modes have different vibration modes. Therefore, when research is carried out for excitation methods of ultrasonic guided wave in the rail, it is necessary to divide

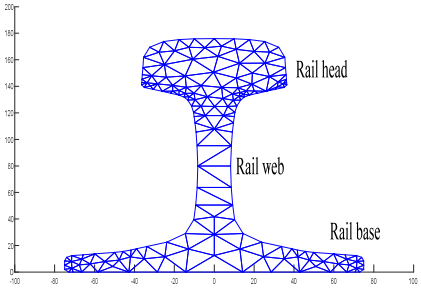

FIGURE 11. Schematic diagram of rail cross section.

cross section of the rail into rail head, rail web, and rail base so as to research vibration features of ultrasonic guided wave modes in three segments in cross section of the rail. There are 35 nodes outside rail head, 22 nodes outside rail web, and 40 nodes outside rail base. The cross section of the rail in each segment is shown in Fig. 11.

Based on vibration features of modes to be excited in three cross segments of the rail, the size of excitation signal will be determined. Therefore, the excitation coefficient γ is introduced and a certain proportion of the excitation signal will be applied for three cross segments of the rail.

There are p nodes outside cross section of the rail and q nodes outside rail base. When the mode m is at rail base, the excitation coefficient RB_γ_{m} is:

$$RB\_\gamma_{\mathrm{m}} = \frac{\sum_{i=1}^{q} |x_i| + \sum_{i=1}^{q} |y_i| + \sum_{i=1}^{q} |z_i|}{\sum_{j=1}^{p} |x_j| + \sum_{j=1}^{p} |y_j| + \sum_{j=1}^{p} |z_j|} \quad (21)$$

Where, $p = 97$ and $q = 40$.

There are h nodes outside rail web and the excitation coefficient RW_γ_{m} when mode m is at rail web is:

$$RW\_\gamma_{\mathrm{m}} = \frac{\sum_{i=1}^{h} |x_i| + \sum_{i=1}^{h} |y_i| + \sum_{i=1}^{h} |z_i|}{\sum_{j=1}^{p} |x_j| + \sum_{j=1}^{p} |y_j| + \sum_{j=1}^{p} |z_j|} \quad (22)$$

Where, $h = 22$.

There are g nodes outside rail head and the excitation coefficient RH_γ_{m} when mode m is at rail base is:

$$RH\_\gamma_{\mathrm{m}} = \frac{\sum_{i=1}^{g} |x_i| + \sum_{i=1}^{g} |y_i| + \sum_{i=1}^{g} |z_i|}{\sum_{j=1}^{p} |x_j| + \sum_{j=1}^{p} |y_j| + \sum_{j=1}^{p} |z_j|} \quad (23)$$

Where, $g = 35$.

1) DETERMINE THE EXCITATION COEFFICIENT AT 200 Hz

When the frequency is 200 Hz, vibration displacement of 4 modes at rail head, rail web, and rail base will be respectively substituted into Equation (21), (22), and (23) and the calculation results are as follows:

RH-EC: Rail head excitation coefficient, RW-EC: Rail web excitation coefficient, RB-EC: Rail base excitation coefficient

It can be seen from Table 8 that:

As for flexural horizontal mode, the excitation coefficient at rail head is 0.40, the excitation coefficient at rail web is 0.21, and the excitation coefficient at rail base is 0.39.

TABLE 8. Excitation coefficient of rail head, rail web and rail base at 200 Hz.

Mode	RH-EC	RW-EC	RB-EC
Flexural horizontal mode	0.3985	0.2086	0.3929
Flexural vertical mode	0.3647	0.2148	0.4205
Torsional mode	0.3465	0.0932	0.5603
Extensional mode	0.3608	0.2260	0.4132

RH-EC: Rail head excitation coefficient, RW-EC: Rail web excitation coefficient, RB-EC: Rail base excitation coefficient

TABLE 9. Excitation coefficient of rail head, rail web and rail base at 35 kHz.

Mode	RH-EC	RW-EC	RB-EC
Mode 1	6.4977e-07	0.0035	0.9965
Mode3	0.1468	0.7981	0.0551
Mode10	7.9303e-04	0.0284	0.9708

As for flexural vertical mode, the excitation coefficient at rail head is 0.37, the excitation coefficient at rail web is 0.21, and the excitation coefficient at rail base is 0.42.

As for torsional mode, the excitation coefficient at rail head is 0.35, the excitation coefficient at rail web is 0.09, and the excitation coefficient at rail base is 0.56.

As for extensional mode, the excitation coefficient at rail head is 0.36, the excitation coefficient at rail web is 0.23, and the excitation coefficient at rail base is 0.41.

2) DETERMINE THE EXCITATION COEFFICIENT AT 35 kHz

When the frequency is 35 kHz, vibration displacement in mode 1, mode 3, and mode 10 at rail head, rail web, and rail base will be respectively substituted into Equation (21), (22), and (23) and the calculation results are as follows:

It can be seen from Table 9 that:

In mode 1, the excitation coefficient at rail head is 0, the excitation coefficient at rail web is 0, and the excitation coefficient at rail base is 1.

In mode 3, the excitation coefficient at rail head is 0.15, the excitation coefficient at rail web is 0.80, and the excitation coefficient at rail base is 0.05.

In mode 10, the excitation coefficient at rail head is 0, the excitation coefficient at rail web is 0.03, and the excitation coefficient at rail base is 0.97.

C. DETERMINE THE EXCITATION POINTS

It is supposed that there are k modes in the rail under the excitation of specific frequency f, and the covariances of node t and e of mode m in x, y, and z directions at the base of the rail are as follows:

$$RB\_Cov_m(t, e) = \frac{\sum_{s=1}^{3} (t_s - \bar{t})(e_s - \bar{e})}{31} \quad (24)$$

The t_s is the vibration displacement data of node t of mode. The s varies in x, y, and z directions. The $\bar{t}$ is the average value of vibration displacement in x, y, and z directions. The e_s is the vibration displacement data of node e of mode m in x, y, and z directions, and $\bar{e}$ is the average value of vibration displacement in x, y, and z directions.

Therefore, the covariance matrix of mode m of q nodes at the base of the rail is as follows:

$$RB\_Cov_m = \begin{bmatrix} RB\_Cov(1,1) & RB\_Cov(1,2) & \cdots & \cdots & RB_C ov(1,q) \\ RB\_Cov(2,1) & RB\_Cov(2,2) & \cdots & \cdots & RB\_Cov(2,q) \\ & & \ddots & & \\ & & & \ddots & \\ RB\_Cov(q,1) & RB\_Cov(q,2) & \cdots & \cdots & RB\_Cov(q,q) \end{bmatrix} \tag{25}$$

The covariance matrix of mode m of h nodes of rail web is as follows:

$$RW\_Cov_m = \begin{bmatrix} RW\_Cov(1,1) & RW\_Cov(1,2) & \cdots & \cdots & RW\_Cov(1,h) \\ RW\_Cov(2,1) & RW\_Cov(2,2) & \cdots & \cdots & RW\_Cov(2,h) \\ & & \ddots & & \\ & & & \ddots & \\ RW\_Cov(h,1) & RW\_Cov(h,2) & \cdots & \cdots & RW\_Cov(h,h) \end{bmatrix} \tag{26}$$

The covariance matrix of mode m of g nodes of rail head is as follows:

$$RH\_Cov_m = \begin{bmatrix} RH\_Cov(1,1) & RH\_Cov(1,2) & \cdots & \cdots & RH\_Cov(1,g) \\ RH\_Cov(2,1) & RH\_Cov(2,2) & \cdots & \cdots & RH\_Cov(2,g) \\ & & \ddots & & \\ & & & \ddots & \\ RH\_Cov(g,1) & RH\_Cov(g,2) & \cdots & \cdots & RH\_Cov(g,g) \end{bmatrix} \tag{27}$$

The covariance can describe the relationship of average deviation of two variables [26]. If the covariance is positive, the two variables are positively correlated and deviate from the mean in the same direction. If the covariance is negative, the two variables are negatively correlated and deviate from the mean in the opposite direction.

In the covariance matrix of mode m at the rail base, if the covariance is positive, the node with maximum autocovariance is the node with the maximum deviation mean, namely the node with the largest vibration displacement. Consequently, the node is selected as the positive excitation point. If there is a negative in the covariance matrix at the rail base, the two nodes with the smallest covariance are the node with the maximum reverse deviation mean. A point is selected as the reverse excitation point by combination with the vibration characteristics of the mode. The excitation points at the rail web and rail head are selected in the same way.

According to the symmetry of the rail structure, partial modes are suppressed by single point excitation, one-sided symmetric excitation, two-sided symmetric excitation or two-sided anti-symmetric excitation according to the vibration characteristics of the mode when the excitation method is selected.

1) DETERMINE THE EXCITATION POINTS AT 200 Hz

The vibration displacement of 97 nodes of four modes at 200 Hz in x, y, and z directions is substituted into the Equation (25), (26), and (27), respectively, to obtain 12 covariance matrices.

In the covariance matrix of torsional mode at the rail base, the autocovariance of node 1 is the largest, that is, the vibration displacement of the torsional mode at the node is of the largest deviation mean. Consequently, the node is selected as the positive excitation point. There is a negative in the covariance matrix at the rail base, where the covariance of node 33 and node 49 is the minimum. The node 49 is selected as the excitation point by symmetry. In the covariance matrix of rail web, the autocovariance of node 35 is the largest. Consequently, the node is selected as the positive excitation point. There is a negative in the covariance matrix at rail web, where the covariance of node 35 and node 45 is the minimum. Consequently, node 45 is selected as the reverse excitation point. In the covariance matrix of rail head, the autocovariance of node 43 is the maximum. Consequently, the node is selected as the positive excitation point. According to the characteristics of torsional mode, the torsional bending is along the x axis. Consequently, the two-sided anti-symmetrical excitation method is selected. Both sides of the cross section of the rail are symmetric along the z axis, and node 39 is selected as the symmetry point of node 43 at rail head.

The excitation points of other modes are determined as shown in Table 10.

The excitation points of the modes at 200 Hz are shown in Fig 12.

In summary, nodes 43, 45, 25 and 49 for one-sided symmetric positive excitation in y direction are selected for the flexural horizontal mode.

Nodes 17, 37, 45, 7 and 26 for two-sided symmetric positive excitation in z direction are selected for the flexural vertical mode.

Nodes 1, 35 and 49 for two-sided symmetric positive excitation in y direction and node 43, 39 and 45 for negative excitation in y direction are selected for the torsional mode.

Nodes 1, 31, 35, 47, 12 and 21 for symmetric positive excitation in x direction are selected for the extensional mode.

2) DETERMINE THE EXCITATION POINTS AT 35 kHz

The vibration displacement of 97 nodes of 20 modes at 35 kHz in x, y, and z directions is substituted into the Equation (25), (26), and (27) respectively, to obtain

TABLE 10. Excitation points at 200 Hz.

	Flexural horizontal mode	Flexural vertical mode	Extensional mode
RB-AMNP	49	7	1
RW-AMNP	45	45	35
RH-AMNP	43	17	12
Modes' vibration characteristics	One-sided symmetric excitation	Two-sided symmetric excitation	Two-sided symmetric excitation
RB-SNP	-	26	31
RW-SNP	25	37	47
RH-SNP	-	-	21

RB-AMNP: Rail base autocovariance maximum node point, RW-AMNP: Rail web autocovariance maximum node point, RH-AMNP: Rail head autocovariance maximum node point, RB-SNP: Rail base symmetry node point, RW-SNP: Rail web symmetry node point, RH-SNP: Rail head symmetry node point

TABLE 11. Excitation points at 35 kHz.

	Mode 1	Mode 3
RB-AMNP	49	30
RW-AMNP	-	73
RH-AMNP	-	23
Modes' vibration characteristics	Single point excitation	Two-sided symmetric excitation
RB-SNP	-	-
RW-SNP	-	74
RH-SNP	-	-

60 covariance matrices. Since there are a lot of 35 kHz modes, Mode 1, 3 and 10 are selected for analysis.

In the covariance matrix of mode 10 at the rail base, the autocovariance of node 30 is the maximum. That is to say, the deviation the mean of vibration displacement of mode 10 at the rail base at the node is the maximum. Consequently, the node is selected as the positive excitation point. There is a negative in the covariance matrix at the rail base, where the covariance of node 30 and node 51 is the minimum. Consequently, node 51 is selected as the excitation point by symmetry. In the covariance matrix of rail web, the self-covariance of node 35 is the maximum. Consequently, the node is selected as the positive excitation point. According to the characteristics of mode 10, the two-sided anti-symmetrical excitation method is selected. Node 47 is selected from rail web as the symmetry point of node 35. As the excitation coefficient of rail head is 0, the excitation point is no longer selected.

The excitation points of other modes are determined as shown in Table 11.

The excitation points of each mode at 35 kHz are shown in Fig 13.

In summary, node 49 for single-point positive excitation in z direction is selected for mode 1.

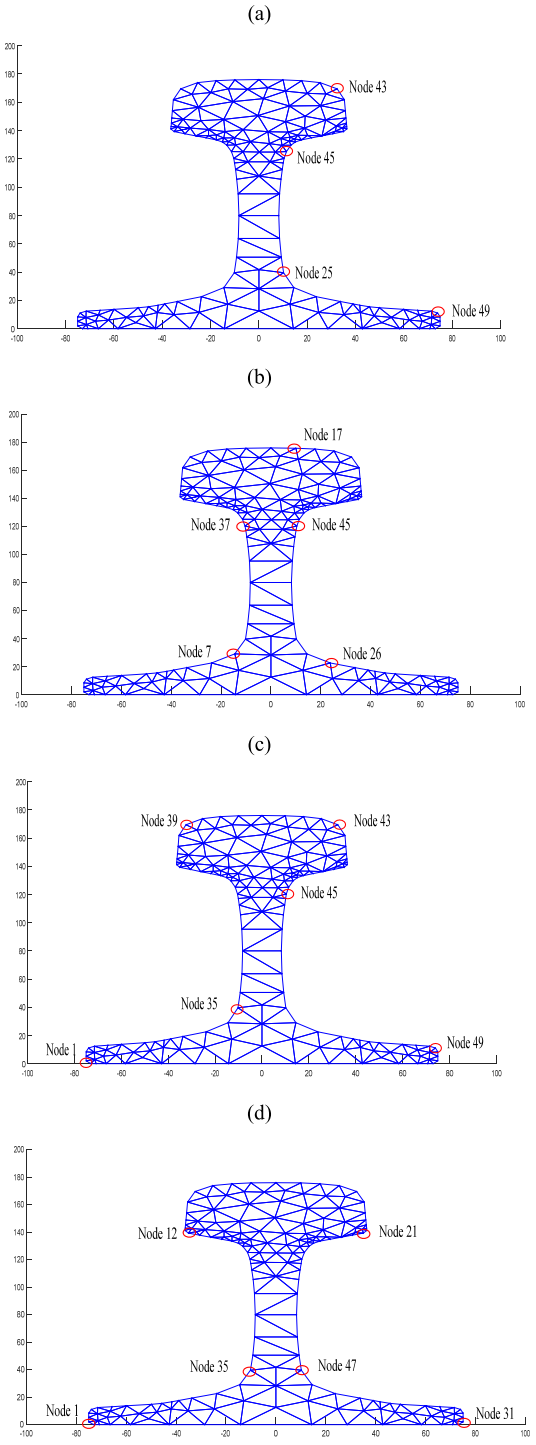

FIGURE 12. Excitation points at 200 Hz. (a) Excitation points of flexural horizontal mode. (b) Excitation points of flexural vertical mode. (c) Excitation points of torsional mode. (d) Excitation points of extensional mode.

Nodes 23, 73, 74 and 30 for one-sided positive excitation in y direction are selected for mode 3.

Node 30 for positive excitation and node 51 for negative excitation in y direction are selected for mode 10 at the rail

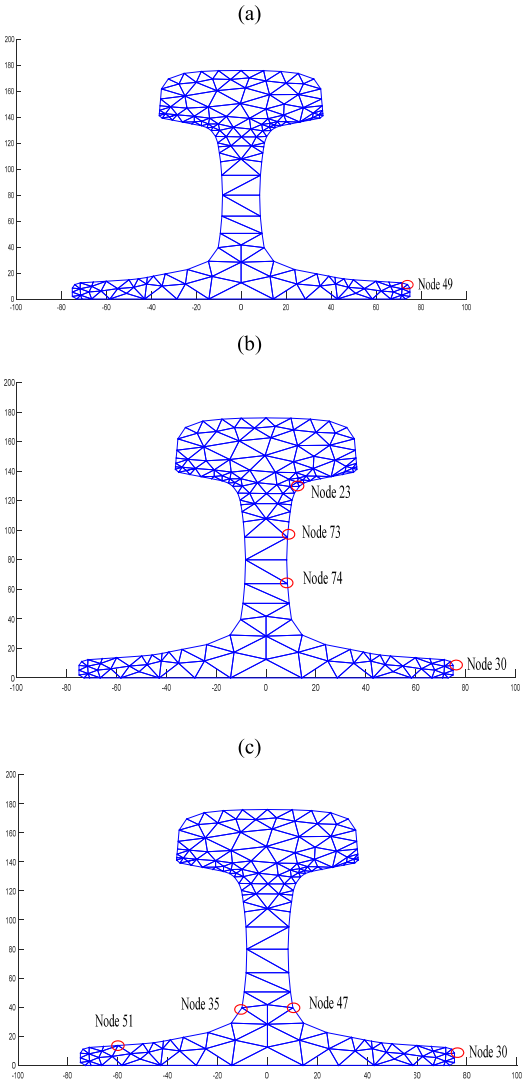

FIGURE 13. Excitation points at 35 kHz. (a) Excitation points of mode 1. (b) Excitation points of mode 3. (c) Excitation points of mode 10.

base, and node 35 and 47 for positive excitation are selected for mode 10 at rail web.

V. SIMULATION RESULTS

After the excitation method of the ultrasonic guided wave mode with low frequency of 200 Hz and high frequency of 35 kHz is determined, the simulation is verified by the SAFE method. In the selected excitation direction, a certain proportion of sine wave modulated by a five-cycle Hanning window is applied to the excitation points selected at the rail head, rail web, and rail base. The excitation signal ratio of rail head, rail web, and rail base are determined by the excitation coefficient. The optimal reception direction of the mode is determined by the simulation results of the excitation response. The mode of the excitation is identified by calculating the simulated group velocity.

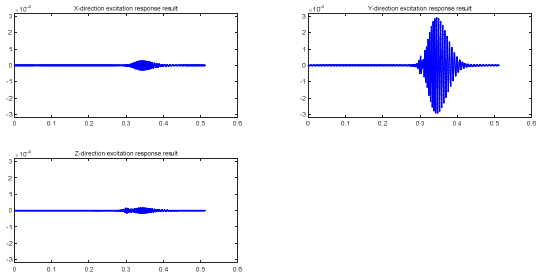

FIGURE 14. Excitation response result of mode 1.

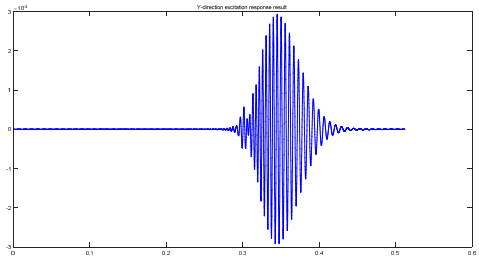

FIGURE 15. Y-direction excitation response result.

A. SIMULATION RESULTS AT 200 Hz

The simulation distance of 200 Hz is 250 meters. The peak of excitation signal appears at 0.01125 seconds.

The one-sided symmetric excitation method is selected for flexural horizontal mode. For node 43, 45, 25 and 49 for positive excitation in y direction, node 49 is selected to receive the signal. The excitation coefficient is 0.40 at rail head, 0.21 at rail web, and 0.39 at rail base. The results of excitation response are shown in Fig 14.

It can be seen that the magnitude of the excitation response in x and y directions is small, and torsional mode also appears in y direction. Therefore, the optimal receiving direction of the excitation signal can be selected by considering the magnitude of the received signal and the interference of other mode. Thus, the optimal receiving direction of flexural horizontal mode excitation signal is y direction and the result is shown in Fig 15.

The two-sided symmetric excitation method is selected for flexural vertical mode. For node 17, 7, 45, 26 and 37 for positive excitation in z direction, node 26 is selected to receive the signal. The excitation coefficient is 0.37 at rail head, 0.21 at rail web, and 0.42 at rail base. The results of excitation response are shown in Fig 16.

The optimal receiving direction of torsional mode excitation signal is z direction and the result is shown in Fig 17.

The two-sided anti-symmetric excitation method is selected for torsional mode. For node 1, 35 and 49 for positive excitation in y direction, and node 39, 45 and 43 for negative excitation in y direction, node 1 is selected to receive the signal. The excitation coefficient is 0.35 at rail head, 0.09 at rail web, and 0.56 at rail base. The results of excitation response are shown in Fig 18.

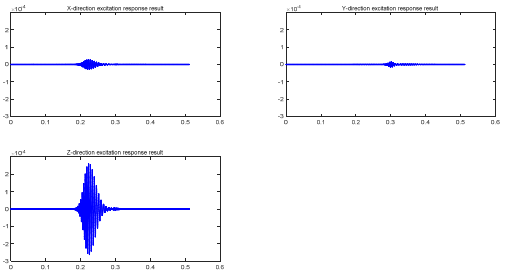

FIGURE 16. Excitation response result of mode 2.

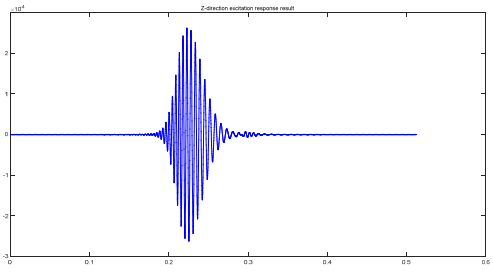

FIGURE 17. Z-direction excitation response result.

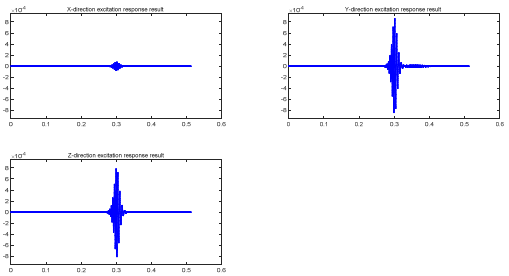

FIGURE 18. Excitation response result of mode 3.

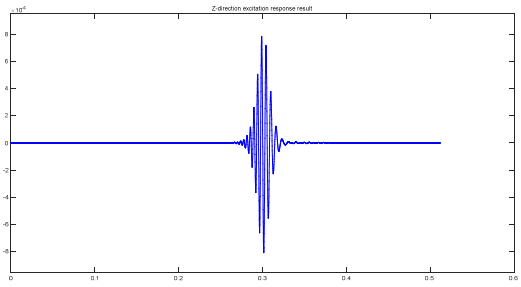

FIGURE 19. Z-direction excitation response result.

The optimal receiving direction of torsional mode excitation signal is z direction and the result is shown in Fig 19.

The two-sided symmetric excitation method is selected for extending mode. For node 1, 31, 35, 47, 12 and 21 for positive excitation in x direction, node 1 is selected to receive the signal. The excitation coefficient is 0.36 at rail head, 0.23 at rail web, and 0.41 at rail base. The results of excitation response are shown in Fig 20.

The optimal receiving direction of extending mode excitation signal is x direction and the result is shown in Fig 21.

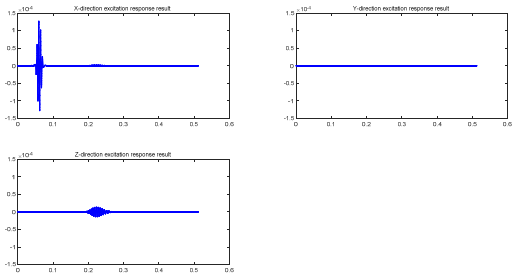

FIGURE 20. Excitation response result of mode 4.

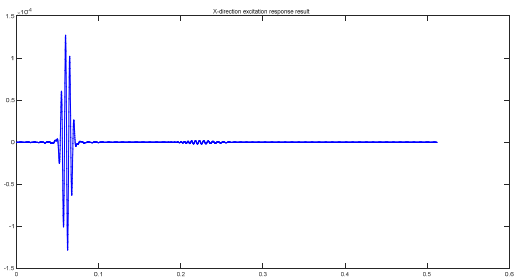

FIGURE 21. X-direction excitation response result.

TABLE 12. Simulation results at 200 Hz.

Mode	ET(s)	RT(s)	SGVV(m/s)	TGVV(m/s)	VD(m/s)
Flexural horizontal mode	0.01125	0.3450	749	772	23
Flexural Vertical mode	0.01125	0.2228	1182	1218	36
torsional mode	0.01125	0.2991	869	886	19
Extensional mode	0.01125	0.0595	5181	5263	82

Excitation time: ET
Response time: RT
Simulation group velocity value: SGVV
Theoretical group velocity value: TGVV
Velocity difference: VD

The group velocity of the mode can be obtained according to the time difference between peak time of mode signal and excitation signal and the simulation distance, as shown in Table 12.

B. SIMULATION RESULTS AT 35 kHz

The simulation distance of 35 kHz is 6 meters. The peak of the excitation signal appears at 6.429e-05 seconds.

Node 49 for single-point excitation in z direction is selected for mode 1 for receiving the signal. The excitation coefficient is 1 at rail base. The results of excitation response are shown in Fig 22.

Considering the magnitude of the received signal and the interference of other modes, the optimal receiving direction of mode 1 excitation signal is z direction and the result is shown in Fig 23.

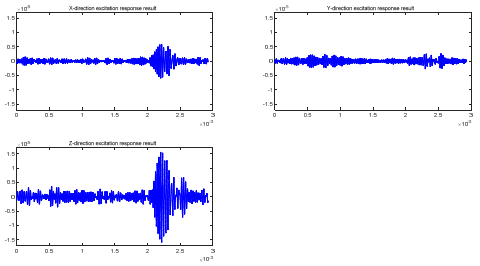

FIGURE 22. Excitation response result of mode 1.

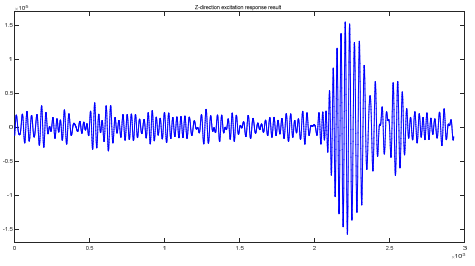

FIGURE 23. Z-direction excitation response result.

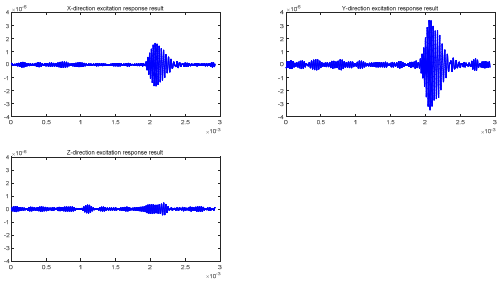

FIGURE 24. Excitation response result of mode 3.

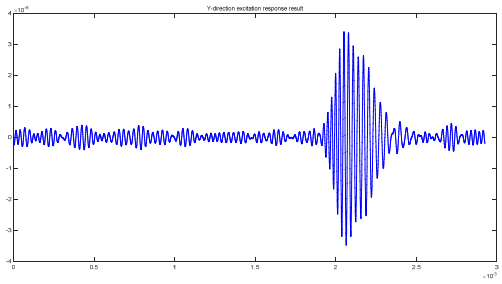

FIGURE 25. Y-direction excitation response result.

The one-sided symmetric excitation method is selected for mode 3. For node 23, 73, 74 and 30 for positive excitation in *y* direction, node 74 is selected to receive the signal. The excitation coefficient is 0.15 at rail head, 0.80 at rail web, and 0.05 at rail base. The results of excitation response are shown in Fig24.

The optimal receiving direction of mode 3 excitation signal is *y* direction and the result is shown in Fig 25.

For node 30 for positive excitation, node 51 for negative excitation in *y* direction and node 35 and 47 for positive excitation in *y* direction, node 30 is selected for mode 10 to receive the signal. The excitation coefficient is 0.03 at rail web and 0.97 at rail base. The results of excitation response are shown in Fig 26.

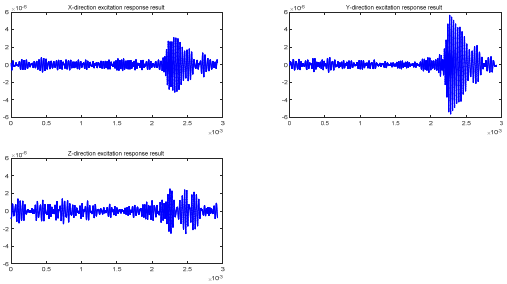

FIGURE 26. Excitation response result of mode 10.

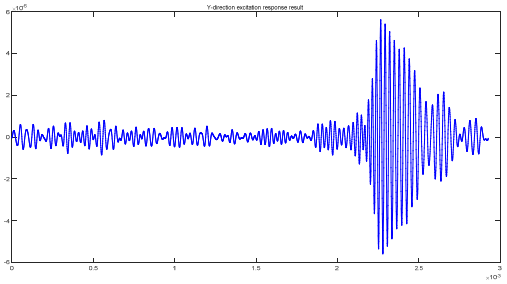

FIGURE 27. Y-direction excitation response result.

TABLE 13. Simulation results at 35 kHz.

Mode	ET(s)	RT(s)	SGVV(m/s)	TGVV(m/s)	VD(m/s)
Mode 1	6.429e-05	0.002203	2805	2853	48
Mode 3	6.429e-05	0.002051	3020	3020	0
Mode 10	6.429e-05	0.002265	2726	2705	22

The optimal receiving direction of mode 3 excitation signal is *y* direction and the result is shown in Fig 27.

The group velocity values of the mode can be obtained according to the time difference between peak time of mode signal and excitation signal and the simulation distance, as shown in Table 13.

It can be seen from the simulation results of excitation response that the expected single mode can be well excited at low frequency of 200 Hz. There is still a partial interference mode at high frequency of 35 kHz, and the expected mode can be received by selecting the optimal direction for reception of excitation signal. The results show that the expected mode can be better excited by determining the excitation direction, excitation coefficient, and excitation node of the target mode in the rail.

VI. CONCLUSION

The ultrasonic guided wave signal provides with the excellent directionality and long propagation distance and it is able to cover the whole cross section of the waveguide.

Therefore, it has considerable advantages in integrity detection and temperature stress measurement of continuously welded rail. However, due to the complex cross-sectional shape of a rail, there are many guided wave modes that can propagate inside and the parameters such as vibration mode and propagation performance of each mode are different. Thus, the premise for non-destructive testing of the rail through guided wave technology is to study the excitation method of each guided wave mode to excite the specific modes. In this paper, the cross-sectional mode shape data of all modes are acquired by using the SAFE method, and the optimum excitation direction of each mode is obtained by Euclidean distance. The cross section of the rail is divided into three segments, including rail base, rail web, and rail head to determine the excitation coefficient of each mode according to the vibration characteristics of each mode in the three cross segments of the rail. Then, the optimum excitation point is calculated by using covariance equation. The correctness of the ultrasonic guided wave excitation method in the rail is better. It is verified by the response results calculated through the calculation method of excitation response with the low frequency of 200 Hz and high frequency of 35 kHz.

ACKNOWLEDGMENT

The authors would like to thank Dr. Wang Rong, for his effective suggestions for data processing. Thanks to Liu Shichao for his help in proofreading this paper.

REFERENCES

[1] J. L. Rose, *Ultrasonic Guided Waves in Solid Media*. Cambridge, U.K.: Cambridge Univ. Press, 2014.
[2] Z. Li, Y. Jiang, C. Hu, and Z. Peng, "Recent progress on decoupling diagnosis of hybrid failures in gear transmission systems using vibration sensor signal: A review," *Measurement*, vol. 90, pp. 4–19, Aug. 2016.
[3] P. Khalili and P. Cawley, "Relative ability of wedge-coupled piezoelectric and meander coil EMAT probes to generate single-mode Lamb waves," *IEEE Trans. Ultrason., Ferroelectr., Freq. Control*, vol. 65, no. 4, pp. 648–656, Apr. 2018.
[4] Z. Liu, J. Fan, C. He, and B. Wu, "Research on baseline-free damage imaging method employing omni-directional S_O mode magnetostrictive transducers," *J. Mech. Eng.*, vol. 51, no. 10, pp. 8–16, 2015.
[5] N. Andruschak, I. Saletes, T. Filleter, and A. Sinclair, "An NDT guided wave technique for the identification of corrosion defects at support locations," *NDT&E Int.*, vol. 75, pp. 72–79, Oct. 2015.
[6] X. Xu, "The basic research on on-line monitoring of stress in continuous welded rails based on ultrasonic guided waves," (in Chinese), School Mech., Electron. Control Eng., Beijing Jiaotong Univ., Beijing, China, Tech. Rep., 2013.
[7] Y. Javadi, M. Hasani, and S. Sadeghi, "Investigation of clamping effect on the welding sub-surface residual stress and deformation by using the ultrasonic stress measurement and finite element method," *J. Nondestruct. Eval.*, vol. 34, no. 1, pp. 1–3, 2015.
[8] S. Liu, Y. Zhang, C. Zhang, and Q. Yang, "Finite element analysis for the inhibition of electromagnetic acoustic testing (EMAT) Lamb waves multimodes," in *Proc. 43rd Rev. Prog. Quant. Nondestruct. Eval.*, vol. 1806, 2017, p. 050014.
[9] S. Patra, H. Ahmed, and S. Banerjee, "Peri-elastodynamic simulations of guided ultrasonic waves in plate-like structure with surface mounted PZT," *Sensors*, vol. 18, no. 1, p. 274, 2018.
[10] W. Zhou, F.-G. Yuan, and T. Shi, "Guided torsional wave generation of a linear in-plane shear piezoelectric array in metallic pipes," *Ultrasonics*, vol. 65, pp. 69–77, Feb. 2016.
[11] X.-W. Zhang, Z.-F. Tang, F.-Z. Lv, and X.-H. Pan, "Excitation of axisymmetric and non-axisymmetric guided waves in elastic hollow cylinders by magnetostrictive transducers," *J. Zhejiang Univ.-Sci. A* vol. 17, no. 3, pp. 215–229, 2016.
[12] H. Miao, Q. Huan, Q. Wang, and F. Li, "Excitation and reception of single torsional wave $T(0,1)$ mode in pipes using face-shear d24 piezoelectric ring array," *Smart Mater. Struct.*, vol. 26, no. 2, p. 025021, 2017.
[13] H. Zhao, C. He, L. Yan, and H. Zhang, "Development of a flexible broadband Rayleigh waves comb transducer with nonequidistant comb interval for defect detection of thick-walled pipelines," *Sensors*, vol. 18, no. 3, p. 752, 2018.
[14] S. P. Pelts, D. Jiao, and J. L. Rose, "A comb transducer for guided wave generation and mode selection," in *Proc. IEEE Ultrason. Symp.*, vol. 2, Nov. 1996, pp. 857–860.
[15] B. Wu, W. Zhou, Y. Zheng, and C.-F. He, "Excitation of single mode Lamb wave simulation based on wave structure," *Nondestruct. Test.*, vol. 33, no. 7, pp. 1–4, 2011.
[16] H. E. C. Huyg and J. P. Jiao, "Array of fundamental torsional mode EMATs and experiment in thick-wall pipe with small diameter," *J. Mech. Eng.*, vol. 51, no. 2, pp. 14–20, 2015.
[17] H. Cunfu, Z. Huamin, L. Yan, and Z. Mingfang, "New type of flexible comb Rayleigh wave sensor based on the PZT," *Chin. J. Sci. Instrum.*, vol. 38, no. 7, pp. 1675–1682, 2017.
[18] H. Kannajosyula, C. J. Lissenden, and J. L. Rose, "Analysis of annular phased array transducers for ultrasonic guided wave mode control," *Smart Mater. Struct.*, vol. 22, no. 8, p. 085019, 2013.
[19] C. Borigo, J. L. Rose, and F. Yan, "A spacing compensation factor for the optimization of guided wave annular array transducers," *J. Acoust. Soc. Amer.*, vol. 133, no. 1, pp. 127–135, 2013.
[20] J. Li and J. L. Rose, "Implementing guided wave mode control by use of a phased transducer array," *IEEE Trans. Ultrason., Ferroelectr., Freq. Control*, vol. 48, no. 3, pp. 761–768, May 2001.
[21] J. L. Rose, "A baseline and vision of ultrasonic guided wave inspection potential," *J. Pressure Vessel Technol.*, vol. 124, no. 3, pp. 273–282, 2002.
[22] T. Hayashi, W. J. Song, and J. L. Rose, "Guided wave dispersion curves for a bar with an arbitrary cross-section, a rod and rail example," *Ultrasonics*, vol. 41, no. 3, pp. 175–183, 2003.
[23] I. Bartoli, A. Marzani, F. L. di Scalea, and E. Viola, "Modeling wave propagation in damped waveguides of arbitrary cross-section," *J. Sound Vib.*, vol. 295, nos. 3–5, pp. 685–707, 2006.
[24] I. Bartoli, A. Marzani, H. Matt, F. L. di Scalea, and E. Viola, "Modeling wave propagation in damped waveguides of arbitrary cross-section," in *Nondestructive Evaulation for Health Monitoring and Diagnostics*, vol. 295. International Society for Optics and Photonics, 2006, pp. 685–707.
[25] G. Xuan, "An Euclidean distance feature selection method in pattern recognition," *Comput. Appl. Softw.*, vol. 2, no. 6, p. 5, 1985.
[26] M.-W. Xie, "The relation of covariance, correlation coefficient and correlation," *Appl. Stat. Manage.*, vol. 23, no. 3, pp. 33–36, 2004.

XU XINING received the Ph.D. degree from the School of Mechanical, Electronic and Control engineering, Beijing Jiaotong University, in 2014. Then, he joined the China Academy of Railway Sciences as a Post-Doctoral Fellow for two years. He has been with the School of Mechanical, Electronic and Control engineering, Beijing Jiaotong University, as a Lecturer, since 2015. He is mainly involved in the research of non-destructive testing technology for high-speed railway infrastructure.

ZHUANG LU received the bachelor's degree from Beijing Jiaotong University in 2017, where she is currently pursuing the M.S. degree with the School of Mechanical and Electronic Control Engineering. Her research interests include ultrasonic-guided wave mode excitation and identification in rails.

XING BO received the bachelor's degree from Beijing Jiaotong University in 2014, where she is currently pursuing the Ph.D. degree with the School of Mechanical, Electronic and Control Engineering. Her present research interests include nondestructive detection of railway infrastructure.

YU ZUJUN received the Ph.D. degree from Beijing Jiaotong University in 2008. He has been a Professor with Beijing Jiaotong University since 2012. He has long been involved in research and teaching in the field of rail transit safety monitoring technology. He has received a number of awards. One of his textbooks was named Beijing fine textbooks in 2013. In 2014, he received the Second Prize of National Graduate Teaching, the New Century Excellent Talents of the Ministry of Education, two Provincial and Ministerial Science and Technology First Prizes, the 2014 Mao Yisheng Railway Technology Award, and the 13th Zhan Tianyou Railway Science and Technology Award–Achievement Award. His present research interests include measurement and control system design.

ZHU LIQIANG received the bachelor's and master's degrees from Beijing Jiaotong University, Beijing, China, in 1994 and 1998, respectively, and the Ph.D. degree from Arizona State University, Tempe, AZ, USA, in 2004. He is currently an Associate Professor with the School of Mechanical, Electronic and Control Engineering, Beijing Jiaotong University. His current research interests include intelligent information processing technologies and safety inspection for rail infrastructure.